LWT - Food Science and Technology 154 (2022) 112786

Contents lists available at ScienceDirect

LWT

journal homepage: www.elsevier.com/locate/lwt

Chemometric approaches to evaluate the substitution of synthetic food dyes by natural compounds: The case of nanoencapsulated curcumin, spirulina, and hibiscus extracts

Valéria Maria Costa Teixeira [a], Roberta França Gomes da Silva [b], Odinei Hess Gonçalves [a,b,c], Carla Pereira [c], Lillian Barros [c], Isabel C.F.R. Ferreira [c], Evandro Bona [a,b], Fernanda Vitória Leimann [a,b,c,*]

[a] Programa de Pós-Graduação em Tecnologia de Alimentos (PPGTA), Universidade Tecnológica Federal do Paraná (UTFPR), Campus Campo Mourão, 87301-899, Campo Mourão, PR, Brazil
[b] Departamento Acadêmico de Alimentos e Engenharia Química (DAAEQ), Universidade Tecnológica Federal do Paraná (UTFPR), Campus Campo Mourão, 87301-899, Campo Mourão, PR, Brazil
[c] Centro de Investigação de Montanha (CIMO), Instituto Politécnico de Bragança, Campus de Santa Apolónia, 5300-253, Bragança, Portugal

ARTICLE INFO

Keywords:
Mixture design
Principal component analysis
Food color
Natural dyes
Synthetic dyes substitution

ABSTRACT

Finding natural food coloring options from plant-based sources to substitute artificial dyes is a challenging task because natural dyes often present low water-solubility, not very vibrant hues, and instability due to interactions with food ingredients. Chemometric approaches can be used to evaluate color differences and patterns resulting from natural and synthetic dyes when applied to food systems. Here, the Mixture Design and the Principal Component Analysis (PCA) were applied to evaluate the substitution of the following artificial food dyes: yolk yellow, apricot yellow, strawberry red, and tartrazine by natural dyes (water-soluble curcumin, yellow shade; *Hibiscus sabdariffa* extract, red shade; *Spirulina platensis* extract, blue/green shade), in three food simulated systems (phosphate buffer, pH 6.9; yogurt, pH 4.0 and citrate buffer, pH 3.0). The color parameters L*, a*, b*, C* and °h were determined and color difference (ΔE*) with artificial dyes resulted in 11 empirical models. PCA yielded a clear map for the identification of the closely matches natural/artificial dyes for the food simulated systems in three subregions. Furthermore, the antioxidant capacity of the natural dyes was determined by OxHLIA and TBARS. It was possible to make an assessment guide that may be useful for other food systems and dyes.

1. Introduction

The overall worldwide turnover of food coloring agents is nearly 8000 tons per year, and they are widely used in different kinds of foodstuffs like carbonated drinks, salads, juices, ice creams and sweets (Khan et al., 2020). It has been established that color is responsible for 62–90% of the consumer's assessment, making in this way, expertise in food colorants a very profitable activity (Viera et al., 2019). Tartrazine (INS 102), sunset yellow (INS 110) and ponceau 4R (INS 129) are synthetic azo dyes extensively applied in foodstuff, and despite that, several studies have identified the chronic effects that food dyes have on human health (do Nascimento et al., 2020). Azoic derivatives are the most important class of dyes that can be described by the formula: *Ar*–N═N–*R*, where *Ar* is an aromatic derivative and *R* is also an aromatic derivative or another group capable to conjugate with the main characteristic group –N═N–(Leulescu et al., 2018).

Natural food colorants can be classified according to their origin (vegetal, animal, bacterial, fungal, etc.), their hue (red, yellow, purple, blue, green, etc.), or their chemical structure as follows: flavonoid derivatives (anthocyanins), isoprenoid derivatives (carotenoids), nitrogen–heterocyclic derivatives (betalains) (Viera et al., 2019). Several beneficial effects are associated with the consumption of these natural molecules, such as the increase in the resistance of low-density lipoprotein to lipid peroxidation, protection of proteins against oxidation, chelation of transition metals that promote oxidative reactions, and inhibition of enzymes that are involved in oxidative stress (Vinha et al.,

* Corresponding author. Centro de Investigação de Montanha (CIMO), Instituto Politécnico de Bragança, Campus de Santa Apolónia, 5300, Bragança, Portugal
E-mail address: fernandaleimann@utfpr.edu.br (F.V. Leimann).

https://doi.org/10.1016/j.lwt.2021.112786
Received 2 August 2021; Received in revised form 29 October 2021; Accepted 6 November 2021
Available online 23 November 2021

2018).

Efforts have been made to substitute synthetic food dyes with natural alternatives, driven by consumer demand since synthetic dyes consumption are is often associated with hyperactivity in children, and also the allergenicity of synthetic colorants in sensitive populations. Although currently used synthetic colorants have long records of safety evaluations and strict regulations, the food industry is seeking alternatives to meet changing market demands and regulatory restrictions (Sigurdson et al., 2017).

The UK Food Standards Agency (Chapman, 2011) published a guideline document that describes options of available natural food coloring agents' manufacturers looking to replace synthetic food dyes. The document highlights that frequently a single natural food dye may not be used as a direct replacement for one synthetic dye. The use of a blend of food dyes is often required to achieve the best match to synthetic ones.

The effect of the "proportions" between ingredients/components in a formulation can be evaluated through the experimental designs for mixtures (Squeo et al., 2021). The mixture design has already been applied in food systems to evaluate the effect of a natural antioxidants' mixture (tea catechins, carnosine, and α-tocopherol) on the color and lipid stability of beef patties (Liu et al., 2010), the effect of wheat, maca and yacon flours proportions on chocolate cake sensory acceptability (Tormena et al., 2017), the effect of xanthan, carboxymethyl cellulose and κ-carrageenan on the height and textural parameters of formulated acorn flour muffins (Masmoudi et al., 2020), and many others. This encourages the use of experimental designs for mixtures to evaluate the resulting color obtained by blends (or mixtures) of natural food dyes and to compare them to artificial dyes.

Principal Component Analysis (PCA) is also a promising tool for the food sector and one of the most widely used data mining techniques in sciences (e.g. sensory, instrumental methods, chemical data). This approach aims to extract the main orthogonal contributors (principal components) which explain most of the variance of the data matrix analyzed and it is also considered a dimension-reduction technique, that can be used to reduce a large set of variables to a smaller set, that still contains most of the information derived from the original set of variables (Cozzolino et al., 2019).

A strategy to compare colors is the use of the color difference (ΔE*). Instrumental measurement of color can be achieved using colorimeters, that express measured colors using the determined coordinates that can be correlated with human eye-brain perception and give tristimulus values directly (L*: luminosity; a*: green $<0<$ red; and b*: blue $<0<$ yellow) (Pathare, Linus Opara et al., 2013). The ΔE* can be defined as the numerical comparison of a sample's color to the standard and indicates the differences in absolute color coordinates (Konica Minolta, 2020).

In the present work, we propose an approach to evaluate the color difference between a natural food dye blend (nanoencapsulated curcumin, modified by encapsulation to allow its water solubility-yellow shade, *Hibiscus sabdariffa* extract-red shade and *Spirulina platensis* extract-blue/green shade) and synthetic food dyes (yolk yellow, apricot yellow, strawberry red and tartrazine) based on a mixture experimental design, and Principal Component Analysis (PCA).

2. Materials and methods

2.1. Materials

Hibiscus and spirulina were purchased at the local market in Campo Mourão (August 2018) to be used as sources of natural dyes. Curcumin from *Curcuma longa* (Turmeric) powder (≥65%, Sigma Aldrich, St Louis, MO), polyvinylpyrrolidone (PVP, Mw = 40,000 g/mol, Sigma Aldrich, St Louis, MO), Tween 80 and absolute ethanol (P.A., Dinâmica, São Paulo, Brazil) were used to produce curcumin water-soluble dye (nanoencapsulation). Anhydrous monobasic sodium phosphate salts (PA, Vetec Química Fina, Duque de Caxias, Brazil), anhydrous dibasic sodium phosphate (PA, Proquímios, Rio de Janeiro, Brazil), dehydrated sodium citrate (PA, Proquímios, Rio de Janeiro, Brazil) and citric acid monohydrate (PA Proquímios, Rio de Janeiro, Brazil) were used to prepare the buffers. Natural yogurt was purchased at the local market in Campo Mourão (PR, Brazil). Artificial dyes were also purchased in the local market: yolk yellow (containing tartrazine, INS 102 and sunset yellow, INS 110), apricot yellow (containing tartrazine, INS 102), and strawberry red (containing ponceau 4R, INS 129) (Mix Ingredients, Indaiatuba, Brazil). Tartrazine (INS 102) was kindly donated by Duas Rodas Industrial (Jaraguá do Sul, Brazil).

2.2. Curcumin nanoencapsulation

Nanoencapsulation was performed using the solid dispersion method presented by Almeida et al. (2017). Initially, Tween 80 (0.040 g) was dissolved in absolute ethanol (110 mL) under magnetic stirring. Then PVP (0.400 g) and curcumin (0.040 g) were added and then the mixture was taken to an Ultrasound (120W, Fisher Scientific, Pittsburg, PA) in pulse regime (30 s on/10 s pause) at 100% amplitude, using a 1/8′ tip and ice bath for 5 min. Then the mixture was transferred to a glass tray and the solvent was evaporated in a convection oven at 50 °C for at least 5 h and the solid was collected as curcumin nanoparticles (C). A complete characterization (Differential Scanning Calorimetry, Fourier Transform Infrared Spectroscopy, X-Ray Diffractometry, and Dynamic Light Scattering) of the produced nanoparticles has been already reported by Almeida et al. (2017).

2.3. Extractions of spirulina and hibiscus

The methodology for extracting phycocyanin from *Spirulina platensis* was adapted from Silveira et al. (2007). In the case of the hibiscus flowers (*Hibiscus sabdariffa*), the methodology was adapted from Rasheed et al. (2018). Spirulina (15 g) was added to distilled water (750 mL) and the mixture was taken to an Ultra-turrax (IKA T25, Staufen, Germany) at 7000 rpm for 20 min. Then the mixture was centrifuged, the supernatant was vacuum filtered, and finally the extract was lyophilized (Liotop L101, Liobrás, São Carlos, Brazil) thus obtaining the Spirulina extract (S). Hibiscus flowers (7.5 g) were added to distilled water at 85 °C (750 mL) and the mixture was taken to the Ultra-turrax at 7000 rpm for 20 min. After that, the mixture was subjected to vacuum filtration and finally lyophilized to obtain the Hibiscus extract (H).

2.4. Antioxidant capacity

2.4.1. Antihaemolytic activity

The antihaemolytic activity of nanoencapsulated curcumin and extracts was evaluated by the oxidative hemolysis inhibition assay (OxHLIA) as described previously by Lockowandt et al. (2019). Sheep blood samples were collected from healthy animals and centrifuged at 1000×*g* for 5 min at 10 °C. Plasma and buffy coats were discarded and erythrocytes were washed once with NaCl (150 mM) and three times with phosphate-buffered saline (PBS, pH 7.4) (Evans et al., 2013). The erythrocyte pellet was then resuspended in PBS at 2.8% (v/v). Using a flat-bottom 48-well microplate, 200 μL of erythrocyte solution was mixed with 400 μL of either PBS solution (control), antioxidant sample dissolved in PBS, or water (for complete hemolysis). Trolox was used as the positive control. After pre-incubation at 37 °C for 10 min, 2,2′-azobis (2-methylpropionamidine) dihydrochloride (AAPH, 160 mM in PBS, 200 μL) was added and the optical density was measured at 690 nm (UV–Vis Specord 200 spectrophotometer, Analytik Jena, Jena, Germany). After that, the microplate was incubated under the same conditions and the optical density was measured every 10 min at the same wavelength for approximately 400 min (Takebayashi et al., 2012). The percentage of the erythrocyte population that remained intact (P) was calculated according to Equation (1), where S_t and S_0 correspond to the

Table 1
Experimental points of the mixture design applied to evaluate the color of the natural food dyes (*C*-curcumin nanoparticles; H-hibiscus extract; *S*-spirulina extract), and ΔE* results obtained between each experimental point of natural dye composition and the artificial dyes (YY- yolk yellow; SR-strawberry red; AY- apricot yellow; T-tartrazine).

Mixture	C	H	S	ΔE* Phosphate Buffer (pH 6.9)				ΔE* Yogurt (pH 4.0)				ΔE* Citrate Buffer (pH 3.0)			
				YY	SR	AY	T	YY	SR	AY	T	YY	SR	AY	T
1	1.000	0.000	0.000	42.95	43.43	41.13	56.94	33.97	87.98	2.92	3.96	39.29	46.79	23.54	7.26
2	0.000	1.000	0.000	30.28	30.42	37.39	51.82	84.48	19.14	87.75	90.37	33.00	23.72	38.90	54.04
3	0.900	0.000	0.100	51.75	52.35	46.37	62.27	43.02	80.30	16.78	20.14	33.51	35.61	6.99	20.56
4	0.000	0.900	0.100	48.85	49.26	45.89	61.63	89.03	27.33	90.12	92.67	45.92	36.69	44.21	60.63
5	0.000	0.950	0.050	36.74	37.00	39.65	54.86	87.07	23.19	89.32	91.91	43.13	33.86	42.98	59.24
6	0.950	0.000	0.050	44.19	44.61	44.02	59.78	39.28	82.38	11.35	12.86	29.86	31.49	5.63	21.77
7	0.500	0.500	0.000	33.29	34.65	7.95	21.36	34.58	81.26	8.92	11.09	29.10	27.11	16.05	32.67
8	0.450	0.450	0.100	45.40	46.30	33.98	49.63	45.65	76.07	23.68	25.28	36.84	32.91	23.00	39.61
9	0.475	0.475	0.050	38.02	39.13	21.83	37.26	40.08	79.10	16.71	18.37	36.38	32.03	25.06	41.75
9′	0.475	0.475	0.050	41.89	42.80	30.88	46.65	40.39	77.11	17.55	19.38	32.55	28.52	27.52	44.10

optical density of the sample at t and 0 min, respectively, and CH_0 is the optical density of the complete hemolysis at 0 min. The results were expressed as the delayed time of hemolysis (Δt), which was calculated according to Equation (2), where H_{t50} is the 50% hemolytic time (min) graphically obtained from the hemolysis curve of each antioxidant sample concentration.

$$P(\%) = \frac{(S_t - CH_0)}{(S_0 - CH_0)} \times 100 \quad (1)$$

$$\Delta t\ (\text{min}) = H_{t50}(sample) - H_{t50}(control) \quad (2)$$

Δt values were then correlated to the antioxidant sample concentrations (Takebayashi et al., 2012) and results were given as IC_{50} values (μg/mL) at Δt 60, i.e., extract or nanoparticles concentration required to keep 50% of the erythrocyte population intact for 60 min.

2.4.2. Inhibition of lipid peroxidation using thiobarbituric acid reactive substances (TBARS)

The procedure to determine the IC_{50} (concentration providing 50% antioxidant activity) of the extracts and curcumin nanoparticles was described by Barreira et al. (2013). Brains were obtained from porcine (*Sus scrofa*), dissected, and homogenized with a Polytron in ice-cold Tris–HCl buffer (20 mM, pH 7.4) to produce a 1:2 (w/v) brain tissue homogenate which was centrifuged at 3000×*g* for 10 min. An aliquot (0.1 mL) of the supernatant was incubated with the extracts with different concentrations (0.2 mL) in the presence of $FeSO_4$ (10 mM; 0.1 mL) and ascorbic acid (0.1 mM; 0.1 mL) at 37 °C for 1 h. The reaction was stopped by the addition of trichloroacetic acid (28%, w/v, 0.5 mL), followed by thiobarbituric acid (TBA, 2%, w/v, 0.38 mL), and the mixture was then heated at 80 °C for 20 min. After centrifugation at 3000×*g* for 10 min to remove the precipitated protein, the color intensity of the malondialdehyde (MDA)–TBA complex in the supernatant was measured by its absorbance at 532 nm. The inhibition ratio (%) was calculated using Equation (3), where A and B were the absorbance of the control and the sample solution, respectively. IC_{50} was calculated by interpolation from the graph of TBARS formation inhibition percentage against sample concentration.

$$\text{Inhibition ratio } (\%) = \frac{(A - B)}{A} \times 100 \quad (3)$$

2.5. Mixture design

A mixture design was generated by Statistica 13 software (TIBCO Software Inc. 2017; Palo Alto, CA) to evaluate the effect of natural dyes proportion on color parameters. A maximum limit of 10% for spirulina extract (S) was applied, since above this limit the mixtures presented a moss green shade. A duplicate at the central point was obtained, the experimental points are presented in Table 1 and a graphical representation is presented in Figure S1.

2.6. Application of the natural dye mixtures and artificial food dyes in model foods

The mixtures were added to buffer solutions, simulating foods with different pHs (phosphate buffer pH 6.9; citrate buffer pH 3.0) and were also applied to natural yogurt (pH 4.0). The concentration of the dye mixture was defined according to the visual aspect (0.1 g of mixture for 10 mL of buffer or yogurt). The mixtures were stirred gently until the color was homogeneous. The artificial dyes were also solubilized in the buffer solutions and natural yogurt (concentrations were chosen based on previous results). All dyes were applied in triplicate and the average was used for further analysis. For the artificial food dyes, the concentrations applied in all systems were: yolk yellow = 20 μL/mL (liquid dye), apricot yellow = 20 mg/mL (solid dye), strawberry red = 3 μL/mL (liquid dye), tartrazine = 20 mg/mL (solid dye).

2.7. Determination of color parameters

Color parameters (L*, a*, b*, C* and h°) of all samples were determined with a Delta Vista 450G colorimeter (Delta Color) equipped with an accessory for color determination in liquids. The color difference (ΔE*) of each experimental point and the artificial dyes (when applied to the same medium) was calculated using Equation (4), using subscript *n* for natural dye mixture and *a* for artificial dye. Three determinations were taken for each sample and the averages of the readings were used in the analysis of the experimental design.

$$\Delta E^* = \sqrt[2]{\left(L_n^* - L_a^*\right)^2 + \left(a_n^* - a_a^*\right)^2 + \left(b_n^* - b_a^*\right)^2} \quad (4)$$

2.8. Mathematical models

To obtain the mathematical models of color difference (ΔE*), the

experimental data were treated by linear regression in the Statistica 13 software, resulting initially in a Special Cubic Equation, represented by Equation (5).

$$\Delta E^{*} = b_1.C + b_2.H + b_3.S + b_{12}.C.H + b_{13}.C.S + b_{23}.H.S + b_{123}.C.H.S \quad (5)$$

where: ΔE* is the color difference between the natural dye mixture and the synthetic dye; b_i is the linear coefficient of the "*i*" component; b_{ij} is the binary interaction coefficient between "*i*" and "*j*" components; b_{ijk} is the ternary interaction coefficient between "*i*", "*j*" and "*k*" components. Analysis of variance were performed (ANOVA, 95% confidence) to validate the models, considering the regression significance and also the lack of fit of the models. When the regression was significant and there was no lack of fit, the significance (p-value ≤ 0.05) and coefficients of determination (R^2 and R^2_{adj}) were evaluated. The model coefficients were removed in the case they did not present significance. Alternatively, coefficients were kept in the model even if not significant when they led to an improvement of R^2_{adj}.

2.9. Principal Component Analysis

To explore the relationship between artificial dyes and natural dye mixtures in the application mediums, a Principal Component Analysis (PCA) was performed using MATLAB R2021a software (MathWorks Inc., Natick, MA). The experimental results of color parameters (L *, a *, b *, C * and h °) were given in columns and the experimental points in lines (10 × 5). Each column was auto-scaled (mean centered and divided by standard deviation), resulting in a correlation matrix (X^TX). The eigenvalue rule was used to define the new dimention's space, meaning that only the principal components (PCs) with eigenvalues greater than 1 (Bona et al., 2018).

2.10. Statistical analysis

The statistical analysis was applied to antioxidant capacity results and averages compared using Tukey's test at a 5% significance level ($p < 0.05$) using Statistica 13 software (TIBCO Software Inc. 2017; Palo Alto, CA).

3. Results and discussion

3.1. Antioxidant capacity

Nanoencapsulated curcumin, hibiscus, and spirulina extracts presented antioxidant capacity in TBARS and OxHLIA assays, as can be observed in Table 2. Nanoencapsulated curcumin presented the highest antioxidant potential between the natural dyes tested in the present work for both assays, while the spirulina extract was the less effective. Curcumin nanoparticles presented an IC_{50} value 90-fold lower than spirulina extract in the TBARS assay and 20-fold lower in the OxHLIA test. In their work, Freitas et al. (2019) found IC_{50} values for nanoencapsulated curcuminoids equal to 38.2 and 11.9 μg/mL in TBARS and OxHLIA assays, respectively. This difference probably occurred because the authors extracted curcumin from *Curcuma longa* rhizomes and in the present work a commercial purified version of curcumin was used.

Table 2
Antioxidant capacity of curcumin nanoparticles, hibiscus and spirulina extracts in terms of TBARS and OxHLIA (IC50).

Sample	TBARS (IC_{50}; μg/mL)	OxHLIA (IC_{50}; μg/mL) Δt = 60 min
Curcumin nanoparticles	$0.064^{a} \pm 0.004$	$27^{a} \pm 2$
Hibiscus extract	$0.700^{b} \pm 0.030$	$73^{a} \pm 3$
Spirulina extract	$5.800^{c} \pm 0.100$	$550^{b} \pm 61$

[a,b]Averages accompanied by the same letter in the same column do not differ significantly from each other ($p > 0.05$) by Tukey's test.

The OxHLIA assay was also applied by Silva et al. (2019) to characterize the antioxidant capacity of *Spirulina platensis*, the authors found an IC_{50} equal to 0.26 mg/mL at Δt = 60 min. The result obtained in the present work was 2-fold higher, probably due to different cyanobacterium cultivation conditions, as well as different extract obtention.

Jabeur et al. (2019) reported IC_{50} values of 72 and 68 μg/mL for the hydroethanolic and infusion extracts of *H. sabdariffa*. Result obtained in the present study is 100-fold lower, which can be related to the different extraction procedure applied, among other factors that affect plants'composition.

The color difference results determined between the artificial dyes and the color of the natural dye mixtures when applied in phosphate buffer, citrate buffer, and natural yogurt are shown in Table 1. The images of the produced mixtures of natural dyes and also artificial dyes applied to the three tested mediums are presented in Fig. 1. The values determined for the L* parameters, a*, and b* in the media for each artificial dye used in the ΔE* calculations (Equation (1)) are presented in Tables S1, S2 and S3.

According to the results (Table 1) it is possible to observe that most of the artificial dyes when applied on the different mediums (phosphate, citrate buffers, and yogurt) presented the highest ΔE* when compared to the mixtures n° 4, composed by 90% hibiscus extract and 10% spirulina extract and mixture n° 3, 90% nanoencapsulated curcumin and 10% spirulina extract. Still, even in the reduced proportion delimited by restriction of the mixture design (maximum 10%), the spirulina extract significantly hampered the homogenization of the mixtures, causing precipitation and lack of homogeneity in the medium. The phycobilisome that serves as the main photosynthetic light-harvesting antenna complex in cyanobacteria (Adir, 2020) is constituted by the three phycobiliproteins, phycocyanin (blue pigment), allophycocyanin (bluish--green pigment) and phycoerythrin (red pigment) (Faieta et al., 2021) as can be observed in Fig. 2 (a). These phycobiliproteins are water-soluble molecules composed of proteins and chromophores, called phycobilins, covalently bound via cysteine (Pagels et al., 2019). One of the methods applied to purify the phycobiliproteins from spirulina extract is precipitation (Martins et al., 2021). Solutions of phycobiliproteins were found to be stable at pH values in the range 5–9, precipitating at low pH conditions (Arad & Yaron, 1992). Even at pH 6.9, this precipitation effect was observed in the present work, probably due to interactions of the phycobiliproteins from spirulina extract and the phenolic compound present at hibiscus extract and curcumin (Zhang et al., 2020).

On the other hand, when comparing dyes mixtures containing nanoencapsulated curcumin and spirulina extract (n° 3, 6, 8 and 9) in different pH conditions, it can be noted that ΔE* determined in citrate buffer (pH 3.0) was always smaller. At this pH, curcumin presents a yellow color since the keto formation is favored (Fig. 2 (c)), however, under basic conditions, the keto tautomer is changed into the state comprising the mixture of enol and enolate forms (Kim et al., 2021). It is possible that this molecular conformation allowed a better color result, even in the presence of spirulina extract.

Between the evaluated application mediums, higher ΔE* values were found for yogurt, with values up to 90.12. This behavior must be a result of extracts compounds' interaction with yogurt proteins. These interactions between protein−polyphenolic compounds could be both

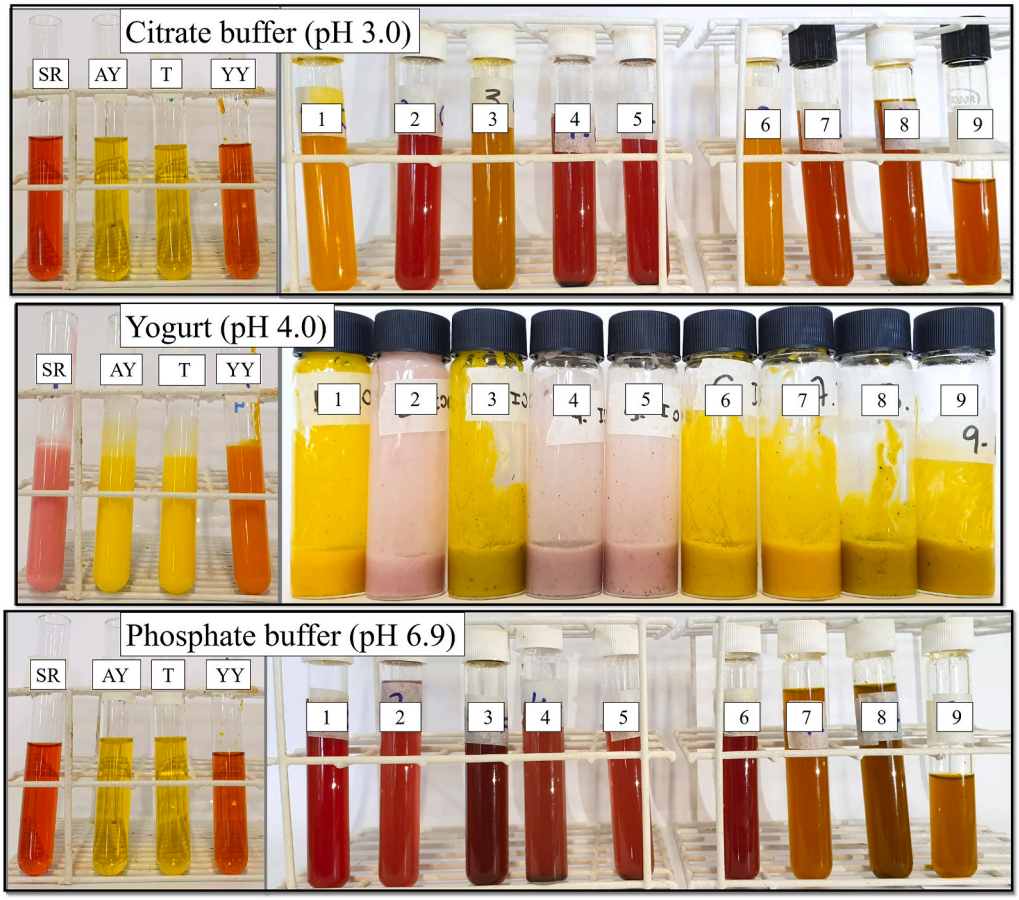

Fig. 1. Images of the artificial dyes (YY- yolk yellow; SR-strawberry red; AY- apricot yellow; T-tartrazine) natural food dyes mixtures (n° 1 to 9) when applied in citrate buffer (pH 3.0), yogurt (pH 4.0) and phosphate buffer (pH 6.9). (For interpretation of the references to color in this figure legend, the reader is referred to the Web version of this article.)

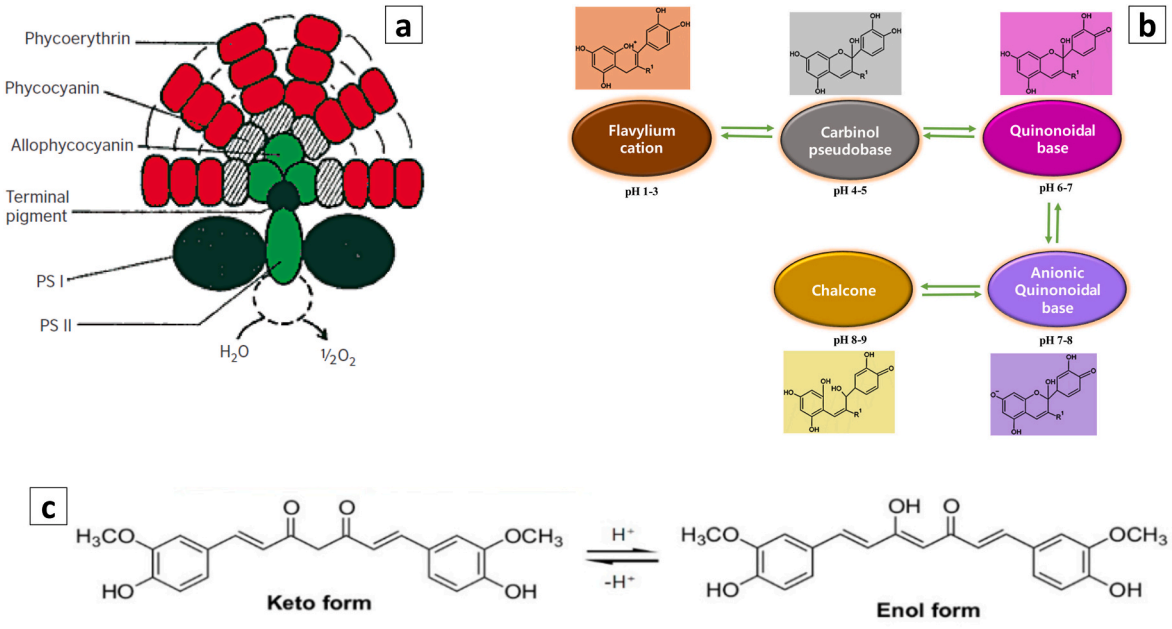

Fig. 2. (a) Structure of Phycobilisome (Gurpreet et al., 2009); (b) pH-dependent chemical structures of anthocyanin. R1-alkoxy group (Castañeda-Ovando et al., 2009); (c) Scheme for the reaction responsible for curcumin color change (Kim et al., 2021). (For interpretation of the references to color in this figure legend, the reader is referred to the Web version of this article.)

Table 3
Coefficients determined for the models related to the ΔE* between natural food dyes mixtures (*C*-curcumin nanoparticles; H-hibiscus extract; *S*-spirulina extract), and the artificial dyes (YY- yolk yellow; SR-strawberry red; AY- apricot yellow; T-tartrazine) when applied at the different mediums (phosphate buffer, citrate buffer and yogurt) (coefficients' p-value between parentheses).

Phosphate buffer (pH = 6.9)				
Coefficients	**YY**	**SR**	**AY**	**T**
C (b_1)	42.35 (<0.01)	42.87 (<0.01)	40.62 (<0.01)	56.15 (<0.01)
H (b_2)	29.63 (<0.01)	29.84 (<0.01)	37.55 (<0.01)	52.32 (<0.01)
S (b_3)	209.01 (<0.01)	210.30 (<0.01)	105.41 (0.02)	127.04 (0.02)
C *x* H (b_{12})	- 12.07 (0.09)	−8.97 (0.18)	−116.45 (<0.01)	−121.64 (<0.01)
C *x* S (b_{13})	- 96.29 (0.07)	−97.77 (0.07)	–	–
H *x* S (b_{23})	–	–	–	–
C *x* H *x* S (b_{123})	–	–	708.12 (0.05)	779.68 (0.05)
p (Regression)	<0.01	<0.01	<0.01	<0.01
p (Lack of fit)	0.80	0.75	0.93	0.90
R^2	96.02	94.87	94.97	94.12
R_{adj}^2	91.05	90.76	90.95	89.95
Citrate buffer (pH = 3.0)				
Coefficients	**YY**	**SR**	**AY**	**T**
C (b_1)	36.84 (<0.01)	43.30 (<0.01)	18.62 (0.01)	8.86 (<0.01)
H (b_2)	33.62 (<0.01)	24.18 (<0.01)	37.25 (<0.01)	53.78 (<0.01)
S (b_3)	175.71 (<0.01)	170.02 (0.01)	−110.14 (0.16)	−2010.44 (0.01)
C *x* H (b_{12})	−16.78 (0.11)	−20.41 (0.12)	−20.07 (0.25)	–
C *x* S (b_{13})	−207.85 (0.02)	−253.81 (0.02)	268.02 (0.06)	2381.47 (<0.01)
H *x* S (b_{23})	–	–	–	2354.53 (<0.01)
C *x* H *x* S (b_{123})	–	–	–	–
p (Regression)	0.03	0.06	<0.01	<0.01
p (Lack of fit)	0.56	0.41	0.21	0.49
R^2	82.67	78.73	90.94	99.16
R_{adj}^2	68.81	61.71	83.7	98.49
Yogurt (pH = 4.0)				
Coefficients	**YY**	**SR**	**AY**	**T**
C (b_1)	34.19 (<0.01)	87.53 (<0.01)	2.87 (<0.01)	3.98 (<0.01)
H (b_2)	84.55 (<0.01)	19.12 (<0.01)	87.70 (<0.01)	90.31 (<0.01)
S (b_3)	4.65 (0.94)	101.03 (<0.01)	−79.41 (0.44)	−93.58 (0.42)
C *x* H (b_{12})	−100.35 (<0.01)	110.76 (<0.01)	−145.09 (<0.01)	−144.11 (<0.01)
C *x* S (b_{13})	131.63 (0.16)	−101.70 (<0.01)	267.52 (0.07)	288.31 (0.08)
H *x* S (b_{23})	137.39 (0.15)	–	211.90 (0.12)	229.79 (0.13)
C *x* H *x* S (b_{123})	–	–	−59.95 (0.13)	−93.38 (0.06)
p (Regression)	<0.01	<0.01	<0.01	<0.01
p (Lack of fit)	0.46	0.90	0.90	0.97
R^2	99.99	99.95	100.00	100.00
R_{adj}^2	99.98	99.91	99.99	99.99

reversible and irreversible depending on pH, temperature, and protein and polyphenolic compound concentration. Furthermore, they can happen at different levels depending on the type of phenolic (Trigueros et al., 2014).

3.2. Mixture design: the color difference between natural mixtures and artificial dyes

Empirical models were determined to describe the color difference between natural mixtures and artificial dyes in citrate and phosphate buffer mediums, as well as in yogurt. Table 3 shows the summarized results of the analysis of variance of the regression of the empirical models for color difference between mixtures and artificial dyes, as well as the coefficients of ΔE* models. The complete ANOVA tables for each model are presented in Tables S4-S15.

According to Table 3, there is no lack of fit for the color difference (ΔE*) between the experimental points and both artificial dyes, yolk yellow, and strawberry red when applied in the phosphate buffer, since the p-value of the lack of fit is greater than 5%. In addition, the regression is significant, as $p < 0.05$. There was also no lack of fit for the apricot yellow artificial dye applied to the same buffer. Furthermore, the regression is significant ($p < 0.05$). The coefficients of pure spirulina extract, as well as the binary interaction factors between the components (b_{12}, b_{13} and b_{23}) were not significant but they were kept in the model to improve prediction power. Also, R^2 and R^2_{adj} were adequate to describe the color difference between the artificial dye and the mixture of natural dyes.

The linear coefficients of the encapsulated curcumin (b_1) and the hibiscus extract (b_2) were significant for the color difference model with the yolk yellow dye in the phosphate buffer (Fig. 1). The linear factor referring to the spirulina extract, as well as the binary interaction factors between the components (b_{12}, b_{13} and b_{23}) were kept in the model to improve data prediction (R^2 and R^2_{adj}). The ternary interaction factor was removed from the model because it was not significant and also compromised predictive capacity. The values of R^2 and R^2_{adj} were adequate to describe the color difference between the artificial dye and the mixture of natural dyes.

All 3 pure components of the mixture had a positive effect on the color difference, and the interaction between the binary components presented a negative effect on the ΔE*. Thus, it is clear that the interactions between the compounds led to a better approximation of the color of the natural compounds in the evaluated medium (phosphate buffer) regarding the artificial dye in question (yellow yolk), as can be seen in Fig. 1. If the pure compound were used isolated, the hibiscus extract would present greater similarity, however, the mixtures still have an advantage by reducing the ΔE*, especially those composed by hibiscus and encapsulated curcumin.

The pure components coefficients (curcumin, hibiscus and spirulina)

were statistically significant for the color difference model for the strawberry red dye in the phosphate buffer (Fig. 1). Only two of the binary interaction factors were kept in the model (b_{12} and b_{13}) to improve data prediction (R^2 and R^2_{adj}) while the ternary interaction factor was removed. The values of R^2 and R^2_{adj} were adequate to describe the color difference between the artificial dye and the mixture of natural dyes. The same behavior determined for the yolk yellow dye was observed for the strawberry red dye, the binary mixture of hibiscus extract and encapsulated curcumin ensured a closer approximation of the color when compared to the artificial dye.

For tartrazine artificial dye, both regression analysis and model coefficients were significant and did not show any lack of fit considering a confidence level of 95%. The only factors that did not show significance at 95% confidence in the model were the binary mixtures in which spirulina extract was present (b_{13} and b_{23}). These factors also did not contribute to model prediction power and were then removed. The ternary interaction factor (b_{123}) presented a p-value at the limit of significance, and its permanence contributed to an improvement in the prediction of the model (R^2 and R^2_{adj}). The greatest significance was found for the mixture of hibiscus extract and curcumin that contribute positively to the reduction of color variation. Again, the interaction between encapsulated curcumin and hibiscus extract provides an approximation of the color of the mixture to the artificial dye, reducing ΔE* (Fig. 1).

As for the results regarding the application of dyes in citrate buffer (Fig. 1) with yolk yellow dye, the regression analysis indicated model significance, and no lack of fit at 95% confidence was detected. The evaluation of the model coefficients indicates that the pure hibiscus extract coefficient was the most significant for the model among the parameters. Also in this model, the factor of the binary mixture of encapsulated curcumin and spirulina extract resulted in a better approximation of the color with the yolk yellow dye.

The encapsulated curcumin can be used in products of any degree of acidity (Guo et al., 2020), and citrate has an acidic pH, which favors the coloration with this compound. On the other hand, the pH between 5.0 and 6.0 is the most adequate to keep the properties of phycocyanin, a compound that gives color to spirulina, while the pH 5.0 leads spirulina extract to low stability (Chaiklahan et al., 2012). At pH 3.0, phycocyanin precipitation and denaturation occurred which is indicated by discoloration (Chaiklahan et al., 2012). Citrate proved to be more adequate to promote the original color of curcumin extract however, it changed the original color of spirulina, resulting in a color closer to the yolk yellow dye. The model for the color difference with the strawberry red artificial dye applied in the citrate buffer did not show significance ($p > 0.05$), and its prediction was inadequate to describe such a response.

There is no lack of fit for the color difference (ΔE*) apricot yellow dye applied in the citrate buffer while regression was significant ($p < 0.05$). Only the coefficients of the encapsulated curcumin and pure hibiscus extract components showed significance at 95% confidence. According to Março and Scarminio (2007) in an acidic medium, anthocyanins present an intense reddish color. But as the pH increases, the anthocyanins lose their color, because when the pH reaches 6.5–8.0, violet-colored structures (anhydrobases) are formed. The interaction of hibiscus and curcumin was not significant in the acidic medium, although the color difference was almost two-fold higher than in the phosphate medium.

For the tartrazine dye in the citrate buffer, it was found that the model was statistically significant ($p < 0.05$) and that there is no lack of fit. Binary interaction factors between encapsulated curcumin and hibiscus extract (b_{12}), and the ternary interaction factor (b_{123}) were eliminated. When compared to the model for tartrazine with the mixture of natural dyes and phosphate buffer, the results for the citrate buffer differed mainly due to binary interaction effects (Fig. 1). For phosphate buffer, only the interaction between encapsulated curcumin and hibiscus extract led to a significant reduction in ΔE*. In the case of citrate buffer, this interaction was not significant, while the two interactions with spirulina (b_{23} and b_{13}) showed significance. Even the most favorable pH for the stability of the phycocyanin molecule being 5.5–6.0, the linear coefficient of spirulina extract was significant for the model in the citrate buffer with pH 3.0, consequently resulting in a decrease in the color difference with tartrazine. Thus, probably, the phycocyanin may have undergone a color variation, suffering a discoloration and the mixture presented a yellowish color, approaching the characteristic color of tartrazine.

The application of dyes in yogurt was also evaluated. For the yolk yellow dye, the model presented significance to describe the color difference data while there was no lack of fit and all coefficients maintained were significant at 95% confidence. The interaction coefficients of the binary mixture of hibiscus and spirulina extracts (b_{23}) were eliminated, as well as the coefficient of the ternary mixture (b_{123}). The model for yogurt showed that the interactions of the encapsulated curcumin with the spirulina extract were important to bring the color of the mixture closer to that of the artificial dye (Fig. 1). Whipped natural yogurt contains skim milk and/or reconstituted skim milk, whole milk and/or reconstituted whole milk, concentrated whey, liquid sugar, modified starch, dairy yeast and gelatin as the stabilizer. These ingredients can influence the color obtained after adding the dyes, as citrate and phosphate buffers do not have these ingredients. Yogurt usually presents dense aggregates of proteins, generated by collisions and shear during the mixing process (Lee & Lucey, 2006), and these proteins help in mixing and better homogenization and absorption of dyes, both natural and artificial. According to the results obtained by Mohammadi-Gouraji et al. (2019), the pH of yogurt and acidity were the most important factors that influenced the color of phycocyanin-enriched yogurt. Authors evaluated b* parameter to confirm the presence of phycocyanin in the yogurt, which can have color variation at pH levels below 4.5 (Chaiklahan et al., 2012; Moreira et al., 2012). However, despite yogurt pH levels found below 4.5, the authors did not find significant changes on b* parameter.

In the case of yogurt, the interaction between encapsulated curcumin and hibiscus extract (b_{12}) was significant and showed greater importance for the model when compared to b_{13}. de Moura et al., 2019 observed that anthocyanin microparticles showed good resistance to the pH of the yogurt matrix (pH 4.75), remaining intact and showing the characteristic color from the obtained extract. This characteristic is of great importance from a technological point of view for bioactive compounds that need to be added to a product with pH different from that on which it presents higher stability. The pH which allows better stability for anthocyanins is 3.0, which is lower than that of yogurt (pH 4.0).

The strawberry red dye when applied to yogurt showed significant regression and did not indicate lack of fit, and all coefficients kept were significant for the model. For application in yogurt, the factor that allowed a better approximation of color was the binary interaction between the encapsulated curcumin and the spirulina extract (b_{13}, Fig. 1). Utpott et al. (2020) observed in their study, that color loss occurred in yogurt added with the unencapsulated extract and similar stability for the yogurts with the encapsulated dye. This suggests that the encapsulated extract is protected when compared to the free extract. The phycocyanin color is associated with the maintenance of the protein structure, therefore, at extreme pH values its structure is denatured (Fukui et al., 2004), so the phycocyanin loses its color at pH below 5.0 and above 7.0, yogurt has a pH of 4.0. Thus, possibly curcumin maintained its original color, while spirulina suffered discoloration due to a pH below the acceptable range for phycocyanins.

The evaluation of the color difference between the apricot yellow dye and the mixture of natural dyes applied in yogurt presented a model with significant regression. There was no lack of fit and all factors were kept in the model. The coefficient that contributed to the closest approximation color mixture to that of the artificial dye was the binary mixture of encapsulated curcumin and hibiscus extract (b_{12}, Fig. 1), a result similar to the behavior determined for the same dye in phosphate

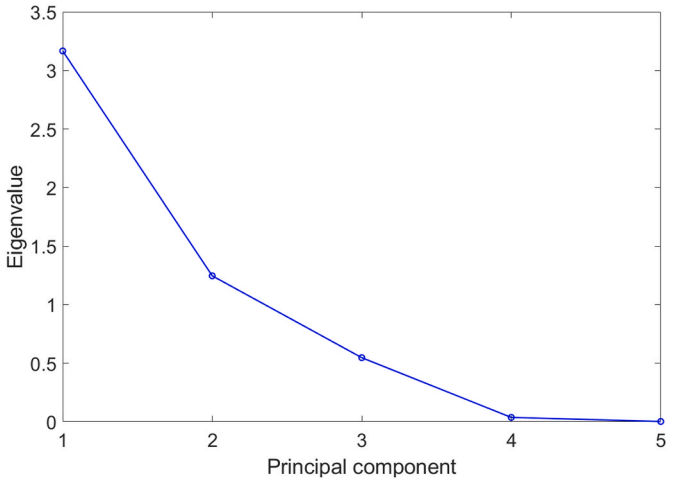

Fig. 3. Scree Plot of experimental color data (L*, a*, b*, C* and h°) of all samples evaluated in the mixture design, as well as artificial dyes in all model foods (citrate, phosphate buffers and yogurt).

buffer.

Finally, for the evaluation of the color difference between the mixture of natural dyes and tartrazine in natural yogurt, it was noted that the model was adequate to describe the experimental data of color difference (significant regression and no lack of fit). All factors were kept in the model to improve prediction power. However, the factor of pure spirulina extract (b_3) was not significant in the case of the model for application in yogurt. According to Lestari and Indrayanto (2014), curcumin has a yellow color at a pH between 1.0 and 7.0 which was the case of phosphate buffer and yogurt. For anthocyanins, compounds that give color to hibiscus in aqueous solutions have different structures depending on pH (Março and Scarminio, 2007). At a pH of approximately 6.0, these compounds gradually lose color until they become practically colorless. Thus, the color of curcumin prevailed, showing greater equivalence to the color of the tartrazine dye.

3.3. Principal Component Analysis

Principal Component Analysis (PCA) was applied to the color parameters (L*, a*, b*, C* and h°) of all samples evaluated in the mixture design, as well as artificial dyes in all model foods (citrate and phosphate buffers, and yogurt). Initially, the number of principal components needed to represent the samples in the new dimensional space was determined. Fig. 3 shows that the first and second PCs attended the eigenvalue rule (Bona et al., 2018). Fig. 3 shows the scores plot of the data set in the dimensional space of PCs 1 and 2. Also in Fig. 4, images referring to the dyes applied to the food models (obtained from Fig. 1) are inserted in the image.

Three clusters of samples were formed. For better identification of experimental points, those composed of a single natural dye (for example, only curcumin or only hibiscus) are described with blue coloring, points composed of binary mixtures in brown, and points of ternary mixtures in magenta. It was observed that the formulations applied to yogurt with pH 4.0 containing the combinations of hibiscus

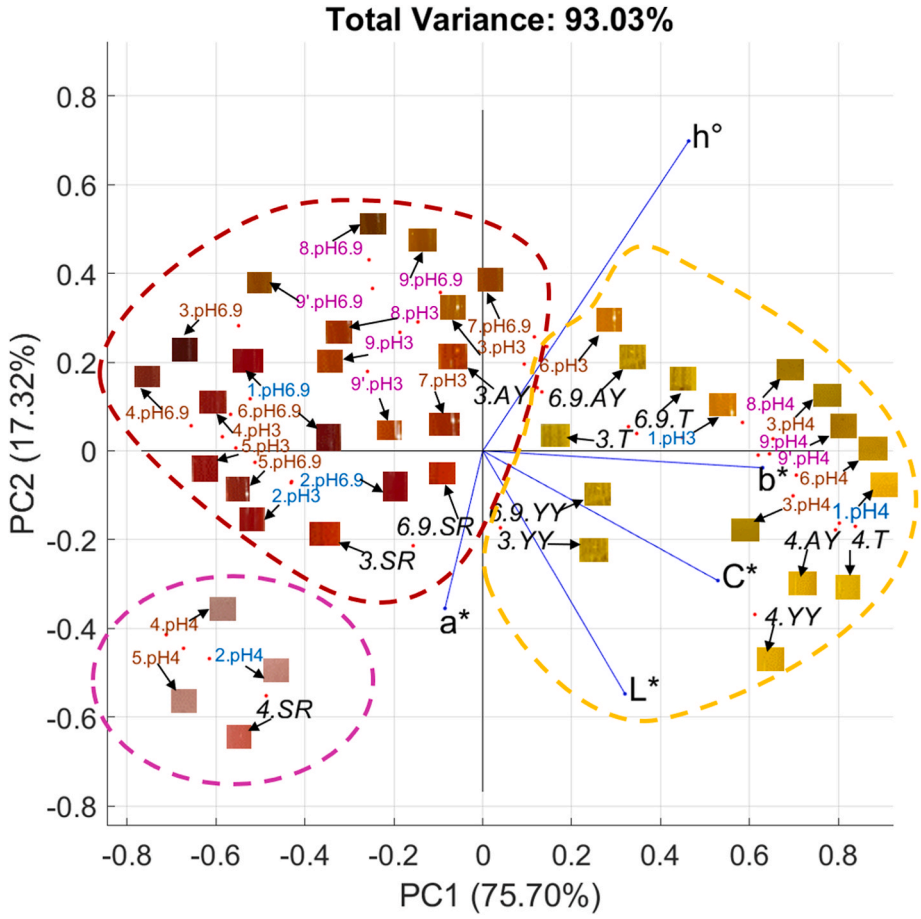

Fig. 4. Biplot for color data of mixtures and artificial dyes for the 3 pHs evaluated. Samples represented by the code equivalent to: experimental point-pH of the medium (example: 4. pH6.9 = mixture of experimental point 4 applied at pH 6.9). Artificial dyes: pH of model food-abbreviation (example: 4. VM = strawberry red dye applied at pH 4). (For interpretation of the references to color in this figure legend, the reader is referred to the Web version of this article.)

and spirulina extracts (Exp. 4 and 5), and pure hibiscus (Exp. 2). These points are located in the group circled in magenta and showed to be more similar to the strawberry red artificial coloring (4. VM). This is probably due to the predominance of the hibiscus extract. These experimental points showed hue angle values lower than 10 and as an alignment of 180° with the vector that describes this parameter. It can be observed in Fig. 3 that the a* parameter is mainly influenced by the negative quadrant of both components. Furthermore, the vector representing the a* parameter is aligned with the group of samples circled in red, indicating that the samples in this group have a reddish color (positive values for this parameter indicate a reddish color). In this group, the experimental point that came closest to the strawberry red artificial dye was point number 2 (100% hibiscus extract).

In the group circled in yellow (Fig. 3), all formulations have a yellowish color (hue angle above 80°) and are directly aligned with the b* vector. It can also be seen in the same group that artificial colors (tartrazine, apricot yellow, and yolk yellow) are aligned with positive chroma and hue angle values. Chroma provides information regarding color saturation or intensity (Cabral-Malheiros et al., 2010; Lawless & Heymann, 1999), and is directly linked to the concentration of the coloring element. The greater the chroma, the greater the saturation of colors that are visible to human eyes. Neutral colors have low saturation, while pure colors have high saturation and are therefore brighter in human perception. The hue angle is a qualitative attribute, such as the definition of reddish, greenish, etc. (Pathare, Opara, & Al-Said, 2013). In addition, it is also noted in this group that artificial coloring when applied to yogurt (pH 4.0) showed higher luminosity values.

In the group characterized by yellowish coloring, the experimental points of the natural dyes that came closest to the attributes of artificial dyes applied at pH 4.0 were points n° 1 (100% curcumin) and n° 3 (90% curcumin and 10% spirulina extract). In the case of tartrazine, when applied in citrate buffer (pH 3.0) and phosphate (pH 6.9) the closest approximation determined was for curcumin encapsulated at 100% (experimental point n° 1) at pH 3.0. Apricot yellow at pH 6.9 showed similarity with experimental point n° 6 at pH 3.0 (95% encapsulated curcumin and 5% spirulina). For the yolk yellow dye in the two buffers (pHs 3.0 and 6.9) the closest natural sample was point n° 3 applied at pH 4.0.

In the group highlighted in red, the artificial colorings apricot yellow, applied in pH 3.0 buffer, and strawberry red in both pH 3.0 and 6.9 can be identified. It was noticed that the samples composed of only hibiscus extract (point n° 2) both at pH 3.0 and at pH 6.9 were the ones that came closest to the characteristics of the strawberry red dye for both pHs. As for the apricot yellow dye at pH 3.0, the closest natural sample was point n° 7 (50% hibiscus extract and 50% encapsulated curcumin) at pH 3.0.

4. Conclusions

Water-soluble curcumin, *Hibiscus sabdariffa* extract, and *Spirulina platensis* extract were used as natural dyes in the substitution of artificial food dyes. The natural dyes presented interesting antioxidant capacity proved by the OxHLIA and TBARS assays, which also encourages their application as health-promoting compounds in substitution to artificial food coloring additives. In addition, the mixture experimental design described the interactions between natural dyes and food pH and also described mathematically the color difference compared to artificial dyes. The Principal Component Analysis allowed the visual description of the proximity between natural dye components and artificial dyes when applied to the different simulated food models. This approach can be used as a reference for color proximity evaluation in other food systems and with other natural or synthetic food dyes.

CRediT authorship contribution statement

Valéria Maria Costa Teixeira: Investigation, (extracts obtention, mixtures production and experimental design evaluation), Formal analysis, Writing – original draft. **Roberta França Gomes da Silva:** Investigation, (curcumin encapsulation and color measurements), Writing – original draft. **Odinei Hess Gonçalves:** Methodology, Formal analysis, Supervision, Writing – review & editing. **Carla Pereira:** Investigation, (antioxidant capacity), Writing – original draft. **Lillian Barros:** Methodology, Formal analysis, Writing – original draft, Supervision. **Isabel C.F.R. Ferreira:** Formal analysis, Writing – original draft, Supervision, Resources, (antioxidant capacity), Funding acquisition. **Evandro Bona:** Conceptualization, Methodology, Formal analysis, Supervision, Writing – review & editing. **Fernanda Vitória Leimann:** Conceptualization, Resources, Writing – review & editing, Supervision, Project administration, Funding acquisition.

Declaration of competing interest

The authors declare that they have no known competing financial interests or personal relationships that could have appeared to influence the work reported in this paper.

Acknowledgments

Authors thank to CNPq (Chamada Universal– MCTI/CNPq N° 28/2018, Process 421541/2018–0) and Fundação Araucária (convênio 039/2019) for the financial support. This study was financed in part by the Coordenação de Aperfeiçoamento de Pessoal de Nível Superior - Brasil (CAPES) - Finance Code 001. Authors thank to Central Analítica Multiusuário da UTFPR Campo Mourão (CAMulti-CM) by the color analysis. Authors are grateful to the Foundation for Science and Technology (FCT, Portugal) for financial support through national funds FCT/MCTES to the CIMO (UIDB/00690/2020). L. Barros and C. Pereira thank the national funding by FCT, P.I., through the institutional scientific employment program-contract for their contracts.

Appendix A. Supplementary data

Supplementary data to this article can be found online at https://doi.org/10.1016/j.lwt.2021.112786.

References

Adir, N. (2020). The phycobilisome. In J. Jez (Ed.), *Encyclopedia of biological chemistry III, 2* pp. 282–290). Elsevier. https://doi.org/10.1016/b978-0-12-809633-8.21539-2.

Almeida, M., da Rocha, B. A., Francisco, C. R. L., Miranda, C. G., Santos, P. D. de F., Araújo, P., Sayer, C., Leimann, F. V., Gonçalves, O. H., & Bersani-Amado, C. C. A. (2017). Evaluation of the *in vivo* acute antiinflammatory response of curcumin-loaded nanoparticles. *Food. Funct., 9*(1), 440–449. https://doi.org/10.1039/C7FO01616F

Arad, S., & Yaron, A. (1992). Natural pigments from red microalgae for use in foods and cosmetics. *Trends in Food Science & Technology, 3*(C), 92–97. https://doi.org/10.1016/0924-2244(92)90145-M

Barreira, J. C. M., Rodrigues, S., Carvalho, A. M., & Ferreira, I. C. F. R. (2013). Development of hydrosoluble gels with *Crataegus monogyna* extracts for topical application: Evaluation of antioxidant activity of the final formulations. *Industrial Crops and Products, 42*(1), 175–180. https://doi.org/10.1016/J.INDCROP.2012.05.034

Bona, E., Março, P. H., & Valderrama, P. (2018). Chemometrics applied to food control. In A. Grumezescu, & A. M. Holban (Eds.), *Food control and biosecurity, 16* pp. 105–133). Elsevier. https://doi.org/10.1016/B978-0-12-811445-2.00004-0.

Cabral-Malheiros, G., Heckttheuer, L. H. R., Canto, M. W., & Balsamo, G. M. (2010). O tempo e o tipo de embalagem sobre a erva-mate tipo chimarrão durante armazenagem em condições ambientais. *Ciência Rural, 40*, 654–660. https://doi.org/10.1590/S0103-84782010005000028

Castañeda-Ovando, A., Pacheco-Hernández, Ma, de L., Páez-Hernández, Ma, E., Rodríguez, J. A., & Galán-Vidal, C. A. (2009). Chemical studies of anthocyanins: A review. *Food Chemistry, 113*(4), 859–871. https://doi.org/10.1016/j.foodchem.2008.09.001

Chaiklahan, R., Chirasuwan, N., & Bunnag, B. (2012). Stability of phycocyanin extracted from Spirulina sp.: Influence of temperature, pH and preservatives. *Process Biochemistry, 47*(4), 659–664. https://doi.org/10.1016/j.procbio.2012.01.010

Chapman, S. (2011). *Guidelines on approaches to the replacement of tartrazine, Allura red, ponceau 4R, Quinoline yellow, sunset yellow and Carmoisine in food and beverages*. UK

Food Standards Agency. Retrieved from https://www.reading.ac.uk/foodlaw/pdf/uk-11026-removing-colours-guidance.pdf. (Accessed 20 March 2021).
Cozzolino, D., Power, A., & Chapman, J. (2019). Interpreting and reporting principal component analysis in food science analysis and beyond. *Food. Anal. Methods., 12*, 2469–2473. https://doi.org/10.1007/s12161-019-01605-5
Evans, B. C., Nelson, C. E., Yu, S. S., Beavers, K. R., Kim, A. J., Li, H., Nelson, H. M., Giorgio, T. D., & Duvall, C. L. (2013). *Ex vivo* red blood cell hemolysis assay for the evaluation of pH-responsive endosomolytic agents for cytosolic delivery of biomacromolecular drugs. *Journal of Visualized Experiments*, (73), 1–5. https://doi.org/10.3791/50166. e50166.
Faieta, M., Neri, L., di Michele, A., di Mattia, C. D., & Pittia, P. (2021). High hydrostatic pressure treatment of *Arthrospira* (*Spirulina) platensis* extracts and the baroprotective effect of sugars on phycobiliproteins. *Innovative Food Science & Emerging Technologies, 70*, 102693–102702. https://doi.org/10.1016/j.ifset.2021.102693
Freitas, P. D., Santos, D., Rafael, C., Francisco, L., Coqueiro, A., Leimann, F. V., Pinela, J., Calhelha, R. C., Porto Ineu, R., Ferreira, I. C. F. R., Bona, E., & Hess Gonçalves, O. (2019). The nanoencapsulation of curcuminoids extracted from *Curcuma longa* L. and an evaluation of their cytotoxic, enzymatic, antioxidant and anti-inflammatory activities. *Food. Funct., 10*, 573–582. https://doi.org/10.1039/c8fo02431f
Fukui, K., Saito, T., Noguchi, Y., Kodera, Y., Matsushima, A., Nishimura, H., & Inada, Y. (2004). Relationship between color development and protein conformation in the phycocyanin molecule. *Dyes and Pigments, 63*(1), 89–94. https://doi.org/10.1016/j.dyepig.2003.12.016
Guo, J., Li, P., Kong, L., & Xu, B. (2020). Microencapsulation of curcumin by spray drying and freeze drying. *Lebensmittel-Wissenschaft und -Technologie, 132*, 109892. https://doi.org/10.1016/j.lwt.2020.109892
Gurpreet, K., Khattar, J. I. S., Singh, D. P., Yadvinder, S., & Jeevesh, N. (2009). Microalgae: A source of natural colours. In J. I. S. Khattar, D. P. Singh, & G. Kaur (Eds.), *Algal Biology and Biotechnology* (pp. 129–150).
Khan, I. S., Ali, M. N., Hamid, R., & Ganie, S. A. (2020). Genotoxic effect of two commonly used food dyes metanil yellow and carmoisine using *Allium cepa* L. as indicator. *Toxicol. Rep., 7*, 370–375. https://doi.org/10.1016/J.TOXREP.2020.02.009
Kim, M., Lee, H., Kim, M., & Park, Y. C. (2021). Coloration and chromatic sensing behavior of electrospun cellulose fibers with curcumin. *Nanomaterials, 11*(1), 222–230. https://doi.org/10.3390/nano11010222
Lawless, H. T., & Heymann, H. (1999). *Sensory evaluation of food: Principles and practices* (2nd ed.). Springer.
Lee, W. J., & Lucey, J. A. (2006). Impact of gelation conditions and structural breakdown on the physical and sensory properties of stirred yogurts. *Journal of Dairy Science, 89*(7), 2374–2385. https://doi.org/10.3168/jds.S0022-0302(06)72310-4
Lestari, M. L. A. D., & Indrayanto, G. (2014). Curcumin. In H. G. Brittain (Ed.), *Profiles of drug substances, excipients and related methodology, 39* pp. 113–204). https://doi.org/10.1016/B978-0-12-800173-8.00003-9
Leulescu, M., Rotaru, A., Ion, P., Moanta, A., Cioatera, N., Popescu, M., Morintale, E., Bubulica, M. V., Florian, G., Harabor, A., & Rotaru, P. (2018). Tartrazine: Physical, thermal and biophysical properties of the most widely employed synthetic yellow food-colouring azo dye. *Journal of Thermal Analysis and Calorimetry, 134*, 209–231. https://doi.org/10.1007/s10973-018-7663-3
Liu, F., Dai, R., Zhu, J., & Li, X. (2010). Optimizing color and lipid stability of beef patties with a mixture design incorporating with tea catechins, carnosine, and α-tocopherol. *Journal of Food Engineering, 98*(2), 170–177. https://doi.org/10.1016/J.JFOODENG.2009.12.023
Lockowandt, L., Pinela, J., Roriz, C. L., Pereira, C., Abreu, R. M. V., Calhelha, R. C., Alves, M. J., Barros, L., Bredol, M., & Ferreira, I. C. F. R. (2019). Chemical features and bioactivities of cornflower (*Centaurea cyanus* L.) capitula: The blue flowers and the unexplored non-edible part. *Industrial Crops and Products, 128*, 496–503. https://doi.org/10.1016/J.INDCROP.2018.11.059
Martins, M., Soares, B. P., M Santos, H. P., Bharmoria, P., Torres Acosta, M. A., R V Dias, A. C., Coutinho, A. P., & M Ventura, S. P. (2021). Sustainable strategy based on induced precipitation for the purification of phycobiliproteins. *ACS Sustainable Chemistry & Engineering, 9*, 3942–3954. https://doi.org/10.1021/acssuschemeng.0c09218
Março, P. H., & Scarminio, I. S. (2007). Q-mode curve resolution of UV–vis spectra for structural transformation studies of anthocyanins in acidic solutions. *Analytica Chimica Acta, 583*(1), 138–146. https://doi.org/10.1016/j.aca.2006.09.057
Masmoudi, M., Besbes, S., Bouaziz, M. A., Khlifi, M., Yahyaoui, D., & Attia, H. (2020). Optimization of acorn (*Quercus suber* L.) muffin formulations: Effect of using hydrocolloids by a mixture design approach. *Food Chemistry, 328*, 127082–127090. https://doi.org/10.1016/J.FOODCHEM.2020.127082
Minolta, K. (2020). Identifying color differences using L*a*b* or L*C*H* coordinates. Retrieved from https://sensing.konicaminolta.us/us/blog/identifying-color-differences-using-l-a-b-or-l-c-h-coordinates/. (Accessed 15 January 2020).
Mohammadi-Gouraji, E., Soleimanian-Zad, S., & Ghiaci, M. (2019). Phycocyanin-enriched yogurt and its antibacterial and physicochemical properties during 21 days of storage. *Lebensmittel-Wissenschaft und -Technologie, 102*, 230–236. https://doi.org/10.1016/j.lwt.2018.09.057
Moreira, I. de O., Passos, T. S., Chiapinni, C., Silveira, G. K., Souza, J. C. M., Coca-Vellarde, L. G., Deliza, R., & de Lima Araújo, K. G. (2012). Colour evaluation of a phycobiliprotein-rich extract obtained from Nostoc PCC9205 in acidic solutions and yogurt. *Journal of the Science of Food and Agriculture, 92*(3), 598–605. https://doi.org/10.1002/jsfa.4614
de Moura, S. C., Schettini, G. N., Garcia, A. O., Gallina, D. A., Alvim, I. D., & Hubinger, M. D. (2019). Stability of hibiscus extract encapsulated by ionic gelation incorporated in yogurt. *Food and Bioprocess Technology, 12*(9), 1500–1515. https://doi.org/10.1007/s11947-019-02308-9
do Nascimento, G. E., Cavalcanti, V. O. M., Santana, R. M. R., Sales, D. C. S., Rodríguez-Díaz, J. M., Napoleão, D. C., & Duarte, M. M. M. B. (2020). Degradation of a sunset yellow and tartrazine dye mixture: Optimization using statistical design and empirical mathematical modeling. *Water, Air, & Soil Pollution, 231*, 231–254. https://doi.org/10.1007/s11270-020-04547-5
Pagels, F., Guedes, A. C., Amaro, H. M., Kijjoa, A., & Vasconcelos, V. (2019). Phycobiliproteins from cyanobacteria: Chemistry and biotechnological applications. *Biotechnology Advances, 37*(3). https://doi.org/10.1016/j.biotechadv.2019.02.010
Pathare, P. B., Linus Opara, U., Al-Julanda Al-Said, F., & A-J Al-Said, F. (2013). Colour measurement and analysis in fresh and processed foods: A review. *Food and Bioprocess Technology, 6*, 36–60. https://doi.org/10.1007/s11947-012-0867-9
Pathare, P. B., Opara, U. L., & Al-Said, F. A. J. (2013). Colour measurement and analysis in fresh and processed foods: A review. *Food and Bioprocess Technology, 6*(1), 36–60. https://doi.org/10.1007/s11947-012-0867-9
Sigurdson, G. T., Tang, P., & Giusti, M. M. (2017). Natural colorants: Food colorants from natural sources. *Annu. Rev. Food Sci. Technol., 8*(1), 261–280. https://doi.org/10.1146/annurev-food-030216-025923
Silveira, S. T., Burkert, J. F. M., Costa, J. A. V., Burkert, C. A. V., & Kalil, S. J. (2007). Optimization of phycocyanin extraction from Spirulina platensis using factorial design. *Bioresource Technology, 98*(8), 1629–1634. https://doi.org/10.1016/J.BIORTECH.2006.05.050
Squeo, G., de Angelis, D., Leardi, R., Summo, C., Caponio, F., & Gonzales-Barron, A. (2021). Background, applications and issues of the experimental designs for mixture in the food sector. *Foods, 10*, 1128–1158. https://doi.org/10.3390/foods10051128
Takebayashi, J., Iwahashi, N., Ishimi, Y., & Tai, A. (2012). Development of a simple 96-well plate method for evaluation of antioxidant activity based on the oxidative haemolysis inhibition assay (OxHLIA). *Food Chemistry, 134*(1), 606–610. https://doi.org/10.1016/J.FOODCHEM.2012.02.086
Tormena, M. M. L., de Medeiros, L. T., de Lima, P. C., Possebon, G., Fuchs, R. H. B., & Bona, E. (2017). Application of multi-block analysis and mixture design with process variable for development of chocolate cake containing yacon (*Smallanthus sonchifolius*) and maca (*Lepidium meyenii*). *Journal of the Science of Food and Agriculture, 97*, 3559–3567. https://doi.org/10.1002/jsfa.8211
Trigueros, L., Wojdyło, A., Sendra, E., Herna, M., & de Beniel km, C. (2014). Antioxidant activity and Protein−Polyphenol interactions in a pomegranate (*Punica granatum* L.) yogurt. *Journal of Agricultural and Food Chemistry, 62*, 6417–6425. https://doi.org/10.1021/jf501503h
Utpott, M., Assis, R. Q., Pagno, C. H., Krigger, S. P., Rodrigues, E., de Oliveira Rios, A., & Flôres, S. H. (2020). Evaluation of the use of industrial wastes on the encapsulation of betalains extracted from red pitaya pulp (*Hylocereus polyrhizus*) by spray drying: Powder stability and application. *Food and Bioprocess Technology, 13*(11), 1940–1953.
Viera, I., Pérez-Gálvez, A., & Roca, M. (2019). *Green. Nat. Colorants. Mol., 24*, 1–17. https://doi.org/10.3390/molecules24010154
Vinha, A. F., Rodrigues, F., Nunes, M. A., & Oliveira, M. B. P. P. (2018). Natural pigments and colorants in foods and beverages. In C. M. Galanakis (Ed.), *Polyphenols: Properties, Recovery, and applications* (pp. 363–391). Elsevier. https://doi.org/10.1016/B978-0-12-813572-3.00011-7.
Zhang, Q., Cheng, Z., Wang, Y., & Fu, L. (2020). Dietary protein-phenolic interactions: Characterization, biochemical-physiological consequences, and potential food applications. *Critical Reviews in Food Science and Nutrition*, 1–26. https://doi.org/10.1080/10408398.2020.1803199